Efficient and multifunctional terahertz polarization control device based on metamaterials*

Xiao-Fei Jiao(焦晓飞)[1,2,3], Zi-Heng Zhang(张子恒)[1,2,3], Yun Xu(徐云)[1,2,3], and Guo-Feng Song(宋国峰)[1,2,3,†]

[1] *Institute of Semiconductors, Chinese Academy of Sciences, Beijing* 100083, *China*
[2] *College of Materials Science and Opto-Electronic Technology, University of Chinese Academy of Sciences, Beijing* 100049, *China*
[3] *Beijing Key Laboratory of Inorganic Stretchable and Flexible Information Technology, Beijing* 100083, *China*

(Received 17 July 2020; revised manuscript received 14 August 2020; accepted manuscript online 9 September 2020)

Terahertz polarization devices are an important part of terahertz optical systems. Traditional terahertz polarization devices rely on birefringent crystals, and their performances are limited by the material structures. In this work, we theoretically demonstrate that the metamaterial consisting of the medium and the periodic metal band embedded in the medium can control broadband polarization effectively. The transmission length of the subwavelength waveguide mode gives rise to a broadband transmission peak. The resonant cavity structure formed by the dielectric layer and the waveguide layer possesses a high transmission efficiency. By optimizing the metamaterial structure parameters, we design a high-efficient ($> 90\%$) quarter-wave plate over a frequency range of 0.90 THz–1.10 THz and a high-efficient ($> 90\%$) half-wave plate over a frequency range of 0.92 THz–1.02 THz. Besides, due to the anisotropy of the structure, the metamaterials with the same structural parameters can achieve the function of the polarized beam splitting with an efficiency of up to 99% over a frequency range of 0.10 THz–0.55 THz. Therefore, the designed metamaterial has a multifunctional polarization control effect, which has potential applications in the terahertz integrated polarization optical system.

Keywords: terahertz, metamaterials, waveguide transmission

PACS: 42.79.Fm, 42.25.Ja, 42.25.Bs **DOI:** 10.1088/1674-1056/abb661

1. Introduction

Polarization is a fundamental characteristic of electromagnetic waves. Polarization-dependent devices are the crucial components in many optical systems. They have a wide range of applications in imaging systems,[1–3] biosensing,[4–6] and communications.[7–9] The traditional polarization controlling method relies on the birefringence effect of optical crystal. Owing to the difference in the refractive index of the optical crystal between orthogonal polarization components during their propagation, a relatively thick device is needed to obtain an enough phase difference thereby controlling the the polarization. The limitations of traditional optical crystals include narrow operating bandwidth, large loss, and large device size. For terahertz waves, the traditional polarization controlling method can no longer keep up with the rapid development of terahertz technology. To overcome these limitations, some artificial structures such as reflective arrays,[10–12] gratings,[13–16] and multilayer structures can be used to achieve terahertz polarization control.[17,18] However, these structures are difficult to achieve in terms of operating bandwidth, efficiency, and optical path design, and have a single function. The alternative to polarization regulation at terahertz frequencies is to use metamaterials. The emergence of metamaterials provides the possibility to solve the above problems.

Metamaterials are new optical materials consisting of arrays of periodic sub-wavelength structures. Due to their unique ability to regulate and control electromagnetic fields, they have attracted much research attention. This new type of artificial material mainly flexibly controls the optical response characteristics of metamaterials by designing the structure, material, and size of the sub-wavelength array to control the characteristics of the optical field amplitude, phase, and polarization. In the previous researches, metamaterials with various functions have proven to be able to manipulate the light field from microwave to ultraviolet band. It is particularly crucial to manipulate the light regulation in the terahertz frequency. In the terahertz frequency range, natural materials have weaker responses to terahertz waves and higher losses. It is difficult to use natural materials to make terahertz wave control devices. The natural material corresponding to the terahertz band is required to have a relatively long propagation distance to realize the regulation of the terahertz wave. The working band corresponding to the crystalline material is fixed. Natural terahertz materials have the disadvantages of narrow bandwidth, non-adjustability, and bulk. In the

*Project supported by the National Key Research and Development Plan, China (Grant No. 2016YFB0402402), the Strategic Priority Research Program of the Chinese Academy of Sciences (Grant No. XDB43010000), the National Key Research and Development Project, China (Grant No. 2016YFB0400601), the National Basic Research Program of China (Grant No. 2015CB351902), the National Science and Technology Major Project, China (Grant No. 2018ZX01005101-010), the National Natural Science Foundation of China (Grant Nos. 61835011and U1431231), the Key Research Projects of Frontier Science of the Chinese Academy of Sciences (Grant No. QYZDY-SSW-JSC004), and the Beijing Science and Technology Projects (Grant No. Z151100001615042).

†Corresponding author. E-mail: sgf@semi.ac.cn

terahertz band, metamaterials can control the propagation of light waves on the structure surface and the surrounding free space. They also have the advantages of high efficiency, easy preparation, and easy integration. With the rapid development of terahertz technology, metamaterials are ideal candidates for various functional devices in terahertz systems. In recent years, the polarization-related terahertz devices based on metamaterials has been reported. For example, the use of metal resonators to form wave plates,[19–21] planar chiral materials,[22–25] magneto-optical films,[26,27] and multilayer metal metamaterials.[28–30] These researches pave the way for achieving the multifunctional terahertz polarization control.

In this work, we design a metamaterial structure consisting of a metal waveguide array wrapped in a medium. In the structure, the surface plasmon is still excited. The upper and lower medium layer and the waveguide layer of this structure form a resonant cavity structure so that efficient polarization control can be achieved in a wide frequency range. In the metamaterial structure, the effective refractive index difference between the TE and the TM modes corresponding to waveguide transmission is much higher than the birefringence difference in a traditional optical crystal. The width of the medium can adjust the relative phase delay between the TE mode orthogonal polarization component and the TM mode in the metamaterial and the transmission length of the waveguide. Therefore, by optimizing the structural parameters, we can design a high-efficient ($> 90\%$) quarter-wave plate over a frequency range of 0.90 THz–1.10 THz and a high-efficient ($> 90\%$) half-wave plate over a frequency range of 0.92 THz–1.02 THz. Besides, in the low-frequency band (0.10 THz–0.55 THz), when the incident light is of TM polarization, the width of the metal strip is less than the wavelength. Because the Ewald–Oseen field is weak which is generated by electrons, most of the light is transmitted.[31] When the incident light is TE polarization, the electrons move along the length of the grating without restriction, and most of the light is reflected. Using metamaterials with the same structural parameters can achieve the effect of polarization beam splitting, with an efficiency of up to 99%. This versatile polarization control device has many potential applications in terahertz optical systems.

2. Model structure

Figure 1 shows a schematic diagram of a high-efficient, broadband terahertz polarization device. The metamaterial consists of a periodic waveguide array embedded in the dielectric material. The metal material is aluminum, and the dielectric material covering the metal strip is Topas. The width of the metal is $w = 5$ μm, the height is $a = 250$ μm, the spacing of the metal strips is $d = 175$ μm, and the metal strips are arranged periodically in the x direction. The incident wave propagates in the positive direction of the Z axis. The TE polarization incidence means that the polarization of the incident light is parallel to the metal strip, that is, along the Y direction and the TM polarization means that the polarization direction of the incident light is perpendicular to the metal strip, that is, along the X direction. The spectral response of the structure is calculated by the finite element method. Since the length of the structure in the Y direction is much larger than the wavelength, the calculation unit here is simplified into a two-dimensional model in the XZ plane. Periodic boundary conditions are applied in the X direction, and perfect matching is applied in the Z direction. The dielectric constant of aluminum is cited from Ordal's work,[32] and the refractive index of Topas is taken to be 1.53.[33]

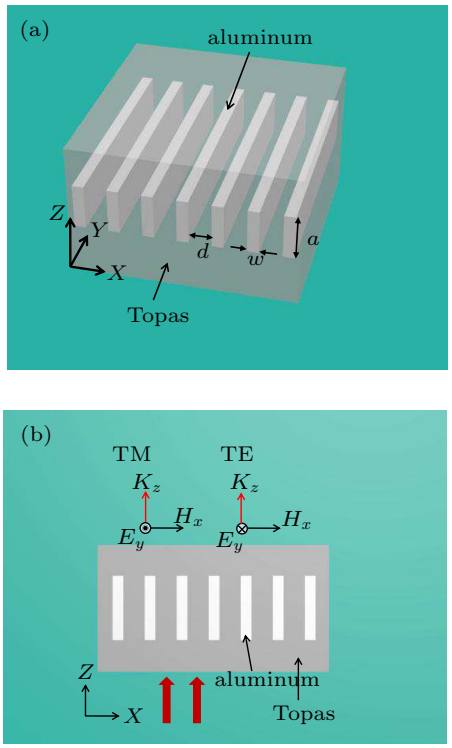

Fig. 1. (a) Three-dimensional schematic diagram of metamaterial, and (b) cross-sectional view of structure in XZ plane.

3. Results and analysis

Under TE and TM polarization incidence, the transmission spectral response of metamaterial is shown in Fig. 2. In the frequency range of 0.80 THz–1.10 THz, the transmittance is higher than 90%.

For better understanding the reason for the high transmittance of the metamaterial structure, we separately analyze the TE- and TM-mode transmissions. In the metamaterial case, the waveguide structure is covered by the dielectric material. The effective refractive index of the waveguide array is different from the refractive index of the upper and lower dielectric material, and the three-layer structure constitutes the resonant cavity. Therefore, Fabry–Pérot (FP) resonance characteristics appear in the transmission spectrum. As shown in Fig. 3, the

transmission peak at a TE incident frequency of 0.85 THz is for low-order FP resonance. There is an asymmetric resonance peak caused by Rayleigh anomaly at 1.06 THz. For the incident wave with a frequency in a range of 0.80 THz–1.20 THz, the corresponding vacuum wavelength is in a range of 375 μm–250 μm. The transmission peak of the FP peak is usually very steep, but the length of the equivalent cavity here is less than the vacuum wavelength, and the corresponding FP resonance order is lower. The TE mode can obtain a higher transmission in a broader frequency range. As shown in Fig. 4(a), for the TE mode, as the waveguide pitch becomes narrower, the resonance peak moves toward the high-frequency range, and high-order FP resonance occurs. As shown in Fig. 4(b), as the transmission distance of the waveguide array becomes longer, the resonance mode corresponding to the FP cavity will move toward a low-frequency direction, and high-order FP resonance will also occur. As the TE incident high-order FP mode gradually approaches to the cut-off wavelength, the transmittance in this mode gradually decreases.

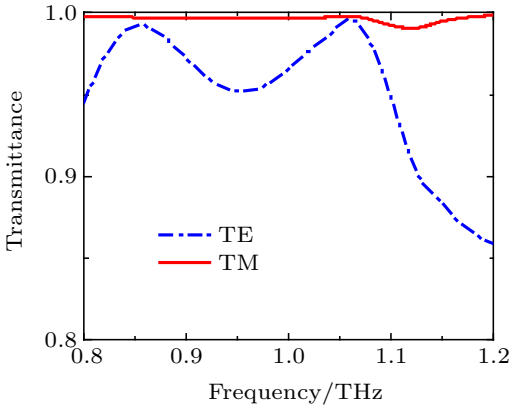

Fig. 2. Metamaterial transmission spectrum under TE and TM polarization incidences.

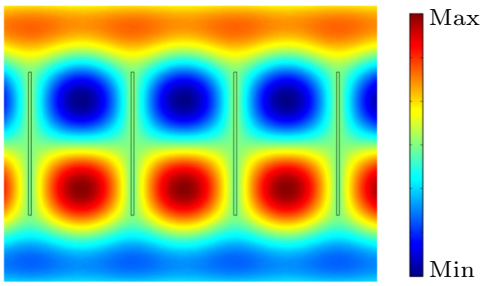

Fig. 3. Electric field distribution in waveguide when TE is incident with waveguide length being 250 μm, metal strip 5 μm, medium width 175 μm, and incident wave frequency 0.85 THz.

For the TM mode, there is no cutoff wavelength. The transmission process of the terahertz wave in the metal waveguide includes the direct transmission of the terahertz wave in the waveguide and the abnormal transmission caused by the surface plasmon polarized wave. When the TM-polarized light passes through the waveguide array, the electric field component perpendicular to the metal surface will excite the surface plasma wave. It will propagate along the metal sidewall to the other end of the waveguide and couple out. Therefore, a part of the TM-polarized light enters into the medium space, and the other part is coupled to the surface plasmon to propagate along the metal surface and finally can

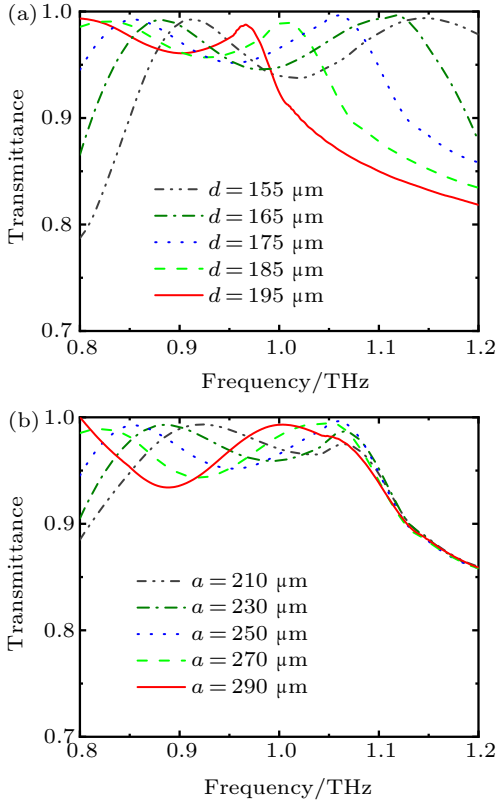

Fig. 4. Plots of TE-polarized light transmittance *versus* frequency for different (a) medium widths and (b) waveguide transmission lengths.

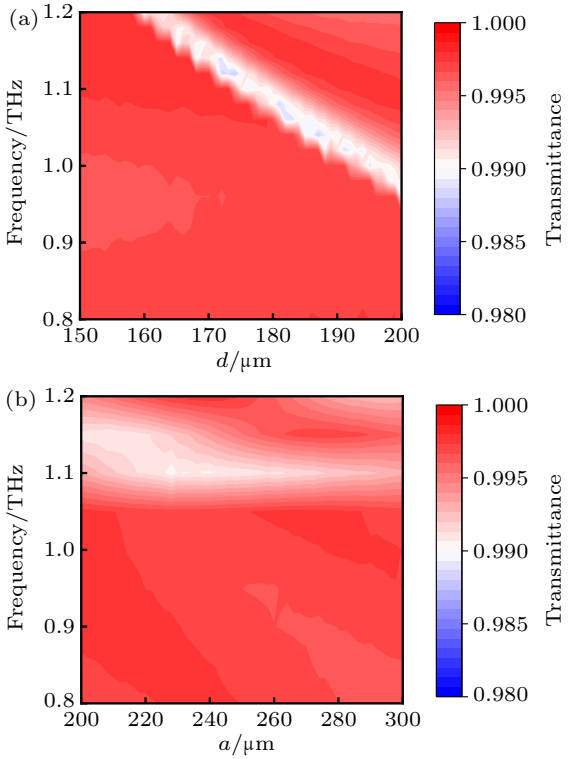

Fig. 5. TM-polarized light frequency *versus* (a) medium widths and (b) waveguide transmission lengths.

propagate along the metal sidewall to the other end of the waveguide. Though the propagation length of the waveguide increases, the TM transmittance does not change much and the TM transmittance has no evident dependence on the medium width d between the metal strips. As shown in Fig. 5, the transmittance of TM is higher than 98%.

In addition to the structural parameters, the dielectric property of the dielectric layer in the structure is also a property that we must discuss. For the TM mode, the refractive index change of the dielectric layer has little effect on the change of its transmittance. Here we focus on TE mode. As shown in Fig. 6, when the refractive index of the dielectric layer increases, the transmission peak moves in the low-frequency direction; when the refractive index of the dielectric layer decreases, the transmission peak moves in the high-frequency direction. This is similar to the dependence of the waveguide mode on the refractive index of the dielectric layer. Therefore, when designing related devices, the refractive index of the medium is one of the factors that must be considered. If a dielectric material with a refractive index different from the refractive index of Topas is used as a dielectric layer, the structural parameters need to be redesigned and optimized. The spectral response of the waveguide cavity is determined by the refractive index and structural parameters of the dielectric layer.

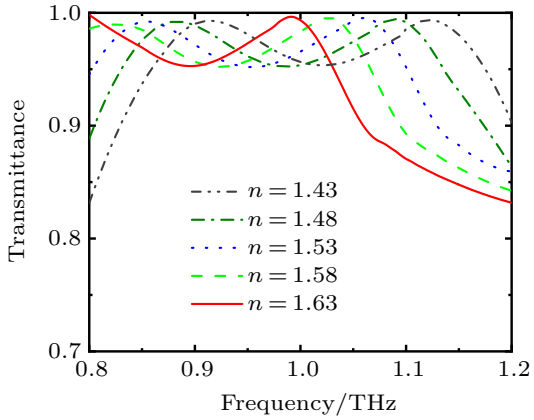

Fig. 6. Plot of TM-polarized light transmittance *versus* frequency at different medium refractive indices.

For a quarter-wave plate, it is necessary to satisfy that the amplitude ratio of the orthogonal polarization component is within 1 ± 0.1, and the transmission phase difference between the orthogonal polarization components is within $90° \pm 10°$.[34] As shown in Fig. 7(a), in the range of 0.90 THz–1.10 THz, the transmittance of TE- and TM-polarized incidences both exceed 90%, and the transmission phase difference is within $90° \pm 10°$, which fully meets the requirements for quarter-wave plates. To obtain ideal circularly polarized transmitted light, we further confirm the performance of the quarter-wave plate. We verify the polarization properties of the transmitted light through the calculation of the two parameters: ellipse angle and ellipticity. The ellipse angle ζ is used to determine the ellipticity, thereby determining the transmitted light's polarization state. The ellipticity χ is the amplitude ratio of the orthogonal electric field components expressed in formulas (1) and (2):[35]

$$\zeta = \frac{1}{2}\arcsin\frac{2|E_x||E_y|\sin(\Delta\varphi)}{|E_x|^2+|E_y|^2}, \tag{1}$$

$$\chi = \frac{|E_x|}{|E_y|}, \tag{2}$$

where E_x and E_y indicate the electric field amplitudes of the TE- and TM-polarized waves, respectively, and $\Delta\varphi$ represents the phase difference.

We can see that in the frequency range of 0.90 THz–1.10 THz, the value of ζ fluctuates in a range from 40° to 45°, and the calculated χ exceeds 0.9 as shown in Fig. 7(b). Therefore, we can draw a conclusion that this metamaterial structure can realize the function of the quarter-wave plate in the above waveband, and can obtain perfect circularly polarized light with an efficiency of more than 90%.

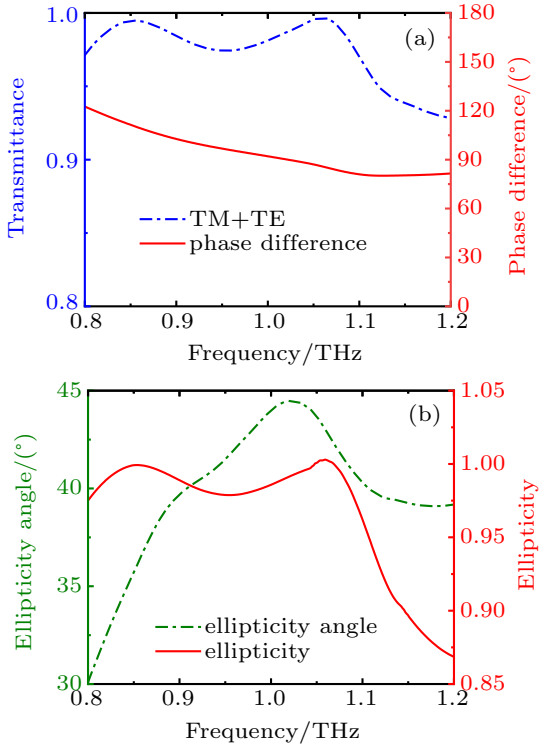

Fig. 7. (a) Plot of linear transmissivity TM + TE and phase difference between electric field components TE and TM *versus* frequency for designed quarter-wave plat. (b) Plot of calculated ellipticity angle ζ and ellipticity χ *versus* frequency.

As the waveguide pitch d decreases, the transmission phase difference between the TE and the TM modes will gradually increase from $\pi/2$ corresponding to the quarter-wave plate to π corresponding to the half-wave plate. Changing the waveguide transmission length a can also change the phase difference between the TE and TM modes. Therefore, an efficient half-wave plate function can be achieved by changing the metamaterial structure parameter metal spacing d or waveguide transmission length a. By further optimizing the

structural parameters of device, we obtain a half-wave plate with high transmittance and broadband operation. We set the structural parameters of the metamaterial to be $a = 290$ μm, $d = 140$ μm, and $w = 5$ μm. It can be seen from Fig. 8(a) that over the frequency range of 0.92 THz–1.02 THz, the amplitude ratio of the orthogonal polarization component is 1 ± 0.1, which is within the allowable range. The value of the phase difference $\Delta\varphi$ in the entire bandwidth is within the range of $\pm 180^\circ \pm 10^\circ$.[36] The transmitted linearly polarized light rotates 90° relative to the incident linearly polarized light. It can also be seen from the sum of the transmittance values of the orthogonal electric field components that the overall efficiency of the half-wave plate we designed over the band range of 0.92 THz to 1.02 THz is higher than 90%. To prove the obtained results more intuitively, we use the following formulas (3) and (4) to calculate the polarization rotation angle Ψ and the linear polarization degree DoLP of the transmitted light:[35]

$$\psi = \frac{1}{2}\arctan\frac{2|E_x||E_y|\cos(\Delta\varphi)}{|E_x|^2 + |E_y|^2}, \tag{3}$$

$$\mathrm{DoLP} = \frac{\sqrt{(|E_x|^2 - |E_y|^2)^2 + (2|E_x||E_y|\cos(\Delta\varphi))^2}}{|E_x|^2 + |E_y|^2}. \tag{4}$$

The polarization rotation angle is defined as the angle between the direction of the transmitted photoelectric field vector and the x-axis direction. The degree of linear polarization is an important parameter used to measure the degree of linear polarization of a light beam. Generally speaking, when the degree of linear polarization is higher than 0.9, we think it is a perfect linearly polarized light. As shown in Fig. 8(b), we can see that the DoLP value of the transmitted light is higher than 0.9 in the frequency range of 0.92 THz–1.02 THz, which shows that the obtained transmitted light is perfect linearly polarized light. Also, it can be seen that the value of Ψ is -45° over the entire bandwidth. Therefore, the designed device has high-efficient half-wave plate performance, and can orthogonally convert the polarization direction of incident linearly polarized light within a 0.10-THz bandwidth.

Generally, the spectral response characteristics based on metal metamaterial strongly depend on the metal material used. It is caused by the difference in the free electron density and effective mass between different metal materials, and the corresponding surface plasmon resonance frequency is changed. However, the realization of the wave plate function in this metamaterial does not rely on surface plasmon resonance. The metal material here only exists as a high-reflection layer, which has an optical limiting effect in the vertical waveguide transmission direction. The optical response of the waveguide resonator is determined solely by the width of the metal strip and the medium's refractive index,and less affected by the type and width of the metal material. So we use cheap metal aluminum materials, and within the allowable range (longer than metal skin depth), the narrower the width of the metal strip, the better the optical response will be.

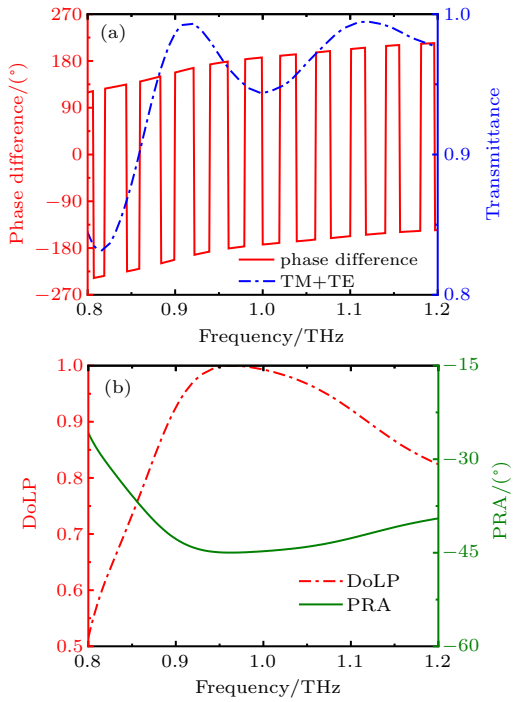

Fig. 8. (a) linear transmissivity TM + TE and phase difference between electric field components TM and TE *versus* frequency for designed half-wave plat. (b) Plot of calculated PRA and DoLP *versus* frequency.

In addition, this metamaterial also has a function of the polarization beam splitting in the low-frequency terahertz band. When the incident frequency is low, the incident light wavelength is much larger than the metal strip pitch. The wavelength of TE mode is longer than the cutoff wavelength of the waveguide mode. In the Y direction, the length of the metal strip is much longer than the wavelength. The electrons move in the Y direction along the metal strip. The conduction electrons are excited and oscillate back and forth, and none of their movements is constrained. The Ewald–Oseen radiation field is generated. The advance directions of the radiated field and the TE wave cancel out. The physical response of this material is similar to that of a thin metal plate. Most of the TE incident light is reflected. For TM, there is no cutoff wavelength, and the width of the metal strip is much smaller than the wavelength, resulting in a feeble Ewald–Oseen radiation field. The electric field polarization of the TM wave is perpendicular to the metal strip, and the surface plasmon mode is excited. It propagates to the other end of the waveguide together with the TM incident wave directly coupled into the waveguide and has a high transmittance. When the metamaterial structural parameters are consistent with the quarter-wave plate ($a = 250$ μm, $d = 175$ μm, $w = 5$ μm), the resulting spectral response results are shown in Fig. 9(b). In the range of 0.10 THz–0.55 THz, both TE reflection efficiency and TM transmission efficiency

rise up to 99%. It can be seen that this metamaterial structure can realize multifunctional terahertz polarization control.

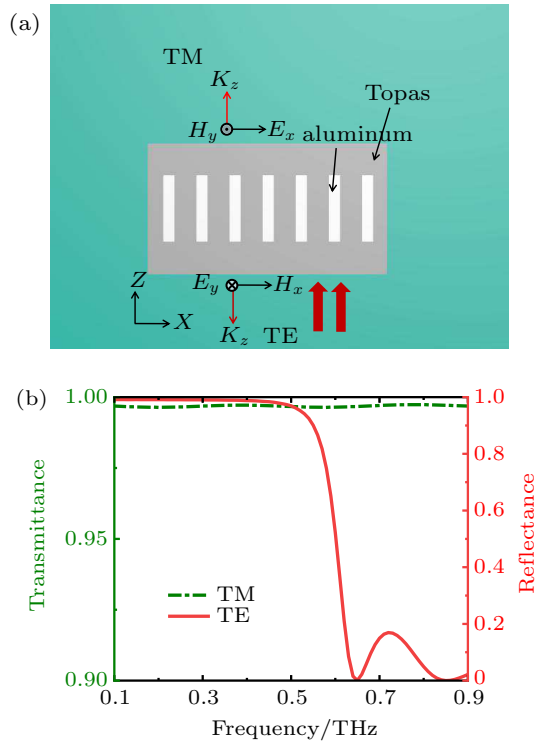

Fig. 9. (a) Schematic diagram of polarization beam splitter. (b) Plot of transmittance and reflectance *versus* frequency for TE and TM incidences.

4. Conclusions

In this work, the metamaterial structure formed by embedding metal strips in the medium realizes the multifunctional polarization control effects such as waveplates and polarization beam splitting. We obtain broadband (0.90 THz–1.10 THz) quarter-wave plates based on the waveguide mode in the metamaterial and improve the efficiency ($>$ 90%) based on the enhanced transmission mode of the resonator. According to the same principle, we design a broadband (0.92 THz–1.02 THz) and high-efficient ($>$ 90%) half-wave plate. Besides, this metamaterial structure has a polarization beam splitting effect over the range of 0.10 THz–0.55 THz, and the efficiency reaches a value as high as 99%. Compared with the polarization control devices of other metal metamaterials, the metamaterial structure in this work possesses the advantage of low requirements for metal materials and dielectric materials, high broadband efficiency and multiple functions, which has broad prospects of applications in polarization modulation in terahertz optical systems.

References

[1] Zallat J, Collet C and Takakura Y 2004 *Appl. Opt.* **43** 283

[2] Yan C, Li X, Pu M, Ma X, Zhang F, Gao P, Liu K and Luo X 2019 *Appl. Phys. Lett.* **114** 161904

[3] Zhang L, Yuan H W and Li X M 2018 *Opt. Quantum Electron.* **50** 353

[4] Alam M Z, Bahrami F, Aitchison J S and Mojahedi M 2014 *IEEE Photonics J.* **6** 3700110

[5] Patskovsky S, Meunier M and Kabashin A V 2008 *Opt. Commun.* **281** 5492

[6] Yu H, Oh Y, Kim S, Song S H and Kim D 2012 *Opt. Lett.* **37** 3867

[7] Core M T 2006 *J. Lightwave Technol.* **24** 305

[8] de Faria G V, Ferreira J, Xavier G B, Temporao G P and von der Weid J P 2008 *Electron. Lett.* **44** 228

[9] Yang H P D, Hsu, I C, Lai F I, Lin G, Kuo, H C and Chi J Y 2007 *Jpn. J. Appl. Phys., Part 2* **46** L326

[10] Carrasco E and Perruisseau-Carrier J 2013 *IEEE Anten. Wirel. Propag. Lett.* **12** 253

[11] Chang Z, You B, Wu L S, Tang M, Zhang Y P and Mao J F 2016 *IEEE Anten. Wirel. Propag. Lett.* **15** 1537

[12] Jia D, Xu J, Xin T, Zhang C and Yu X 2019 *Appl. Phys. Lett.* **114** 101105

[13] Xiao P, Tu X, Kang L, Jiang C, Zhai S, Jiang Z, Pan D, Chen J, Jia X and Wu P 2018 *Sci. Rep.* **8** 8032

[14] Monnai Y, Altmann K, Jansen C, Hillmer H, Koch M and Shinoda H 2013 *Opt. Express* **21** 2347

[15] Xing Q R, Li S X, Zhang W L, Lang L Y, Mao F L, Xu S X, Chai L and Wang Q Y 2005 *Chin. Phys. Lett.* **22** 1821

[16] Zhou S F, Reekie L, Chan H P, Chow Y T, Chung P S and Luk K M 2012 *Opt. Express* **20** 9564

[17] Dubey A, Jain A, Jayalakshmi C G, Shami T C, Awari N and Prabhu S S 2013 *Microw. Opt. Technol. Lett.* **55** 393

[18] Stepanov A G, Rogov A, Bonacina L, Wolf J P and Hauri C P 2014 *Opt. Express* **22** 21618

[19] Liu J, Liang H, Zhang M and Su H 2015 *Opt. Commun.* **339** 222

[20] Nagai M, Mukai N, Minowa Y, Ashida M, Suzuki T, Takayanagi J and Ohtake H 2015 *Opt. Express* **23** 4641

[21] Nagai M, Mukai N, Minowa Y, Ashida M, Takayanagi J and Ohtake H 2014 *Opt. Lett.* **39** 146

[22] Huang Y, Yao Z, Hu F, Liu C, Yu L, Jin Y and Xu X 2017 *Carbon* **119** 305

[23] Shah N A, Ahmad F, Syed A A and Naqvi Q A 2013 *Int. J. Appl. Electromagn. Mech.* **43** 379

[24] Singh R, Plum E, Menzel C, Rockstuhl C, Azad A K, Cheville R A, Lederer F, Zhang W and Zheludev N I 2009 *Phys. Rev. B* **80** 153104

[25] Xu W Z, Shi Y T, Ye J, Ren F F, Shadrivov I V, Lu H, Liang L, Hu X, Jin B, Zhang R, Zheng Y, Tan H H and Jagadish C 2017 *Adv. Opt. Mater.* **5** 1700108

[26] Li T F, Li Y L, Zhang Z Y, Yang Q H, Fan F, Wen Q Y and Chang S J 2020 *Appl. Phys. Lett.* **116** 251102

[27] Li Y L, Li T F, Wen Q Y, Fan F, Yang Q H and Chang S J 2020 *Opt. Express* **28** 21062

[28] Fan K, Strikwerda A C, Zhang X and Averitt R D 2013 *Phys. Rev. B* **87** 161104

[29] Fang B, Cai Z, Peng Y, Li C, Hong Z and Jing X 2019 *J. Electromagn. Waves Appl.* **33** 1375

[30] Yang X, Zhang B and Shen J 2018 *Opt. Quantum Electron.* **50** 315

[31] Juretschke H J 1999 *Am. J. Phys.* **67** 929

[32] Ordal M A, Bell R J, Alexander R W, Long L L and Querry M R 1985 *Appl. Opt.* **24** 4493

[33] Islam M S, Cordeiro C M B, Nine M J, Sultana J, Cruz A L S, Dinovitser A, Ng B W H, Ebendorff-Heidepriem H, Losic D and Abbott D 2020 *IEEE Access* **8** 97204

[34] Zhao Y and Alu A 2011 *Phys. Rev. B* **84** 205428

[35] Li T, Hu X, Chen H, Zhao C, Xu Y, Wei X and Song G 2017 *Opt. Express* **25** 23597

[36] Ding F, Wang Z, He S, Shalaev V M and Kildishev A V 2015 *ACS Nano* **9** 4111